CHEMISTRY OF MATERIALS
Cite This: Chem. Mater. 2020, 32, 121−126
Article
pubs.acs.org/cm

Effect of Chemical Variations in the Structure of Poly(ethylene oxide)-Based Polymers on Lithium Transport in Concentrated Electrolytes

Arthur France-Lanord,[†] Yanming Wang,[†] Tian Xie,[†] Jeremiah A. Johnson,[‡] Yang Shao-Horn,[§] and Jeffrey C. Grossman*,[†]

[†]Department of Materials Science and Engineering, [‡]Department of Chemistry, and [§]Department of Mechanical Engineering, Massachusetts Institute of Technology, Cambridge, Massachusetts 02139, United States

Supporting Information

ABSTRACT: Polymer electrolytes constitute an attractive alternative to current liquid electrolytes used in Li-ion batteries. Unfortunately, the lithium-ion conductivities of the state-of-the-art polymer electrolytes are few orders of magnitude lower than those of liquid electrolytes at room temperature. In this work, we focus on poly(ethylene oxide) (PEO), which has shown the highest lithium ion conductivity in polymer electrolytes so far. At high salt concentrations, the lithium conductivity of a PEO electrolyte is strongly reduced because of the formation of ionic aggregates. Using molecular dynamics simulations and rigorously taking into account ionic correlations, we show how introducing a secondary site with a specific chemical structure in the backbone of PEO can greatly enhance the lithium conductivity of such concentrated electrolytes. In addition, we demonstrate how results based on the Nernst−Einstein equation can be highly misleading in the concentrated regime. We identify PEO-based carbonate and sulfonyl variants that, respectively, allow for significant ion dissociation and high cation transference number.

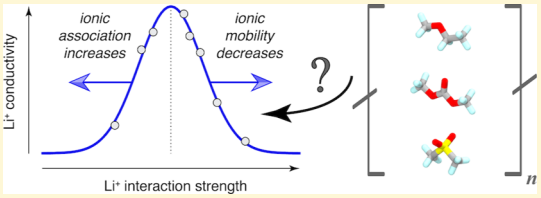

INTRODUCTION

Polymer-based electrolytes represent a potential alternative to current liquid organic solvent-based Li-ion electrolytes,[1,2] with attractive features[3−5] such as improved processability, flexibility, and safety. In addition, they offer greater compliance to accommodate volume changes in the electrode[6] during lithium intercalation/de-intercalation compared to solid inorganic electrolytes.[7] State-of-the-art lithium-ion conducting polymer electrolytes, which are mainly based on poly(ethylene oxide) (PEO),[8] show at best ionic conductivities on the order of 10^{-5} to 10^{-4} S/cm at room temperature.[9,10] Plasticizer additives enable slightly higher conductivities,[11−13] at the expense of the mechanical properties and loss of compatibility with the lithium electrode.[14] This is still 1 to 2 orders of magnitude less than the current liquid organic solvent-based electrolytes.[1] In addition, lithium contributes only marginally to the total conductivity in PEO-based electrolytes, as consistently demonstrated by measurements of the cation transference number t^+,[15,16] that is, the ratio of lithium conductivity to total conductivity. In fact, recent experiments[17] employing the rigorous framework of concentrated solution theory have shown that at high salt concentration—a regime in theory favorable for battery applications due to the increased number of charge carriers—t^+ can be negative for PEO-based electrolytes, which is ascribed to the presence of ionic aggregates.[18−20] Anions do not participate in the electrode chemistries in lithium-based batteries; the performance of an electrolyte with low to negative t^+ for such an application is therefore minimal.[21]

Significant effort has been devoted to enhancing the transport properties of polymer electrolytes, through materials design and exploration.[22−26] One recurrent strategy consists in modifying PEO's chemical structure in a systematic fashion,[14] for example, by adding aliphatic linkers to its backbone.[10] This makes it possible to understand direct structure−property relationships, which allow for the rational design of electrolytes. In this work, we chemically modify PEO with the inclusion of two different secondary sites in the repeating unit of PEO-derived polymers, transforming PEO into an alternating copolymer, which can change fundamental interactions among solvent, anions, and cations governing ion conductivity and lithium transference number. Using classical molecular dynamics simulations, we compute a range of relevant transport properties, including diffusion coefficients, ionic conductivity, and cation transference number. We focus on the high salt concentration regime, where ion interactions cannot be neglected. In this respect, making use of a recently developed method based on cluster analysis,[20] we are able to accurately capture the effects of ionic association and clustering, which are signature features of high salt concentrations. This novel approach allows us to gain detailed

Received: July 3, 2019
Revised: December 3, 2019
Published: December 4, 2019

Downloaded via MASSACHUSETTS INST OF TECHNOLOGY on August 13, 2020 at 15:29:11 (UTC).
See https://pubs.acs.org/sharingguidelines for options on how to legitimately share published articles.

© 2019 American Chemical Society

DOI: 10.1021/acs.chemmater.9b02645
Chem. Mater. 2020, 32, 121−126

insights into the physics of ion transport at play in these electrolytes. From these numerical simulations, we identify two promising PEO variants, with carbonate and sulfonyl secondary sites; the former significantly increasing ion dissociation, and the latter allowing for a high cation transference number. Finally, our work confirms and illustrates how misleading it can be to make the assumption of an ideal solution in the concentrated regime.

■ METHODS

We considered two different secondary sites: a carbonate group (CAR) and a sulfonyl group (SUL), with one EO in each repeating unit of the new polymers. Besides their synthesizability, these chemical species were chosen based on their distinctive electrostatic features, as illustrated in Table 1. These intrinsic characteristics directly influence their interaction with cations and anions and ultimately the electrolyte's transport properties, although in a nontrivial and perhaps somewhat concealed way; these changes have repercussions on the ion's solvation geometry and symmetries, and on the dynamics of the polymer chains themselves, for instance.

Table 1. Structure, Li^+ Binding Energy, Electrostatic Potential (ESP) Map, and ESP Minimum of the Three Chemical Fragments Used to Construct Polymers in This Work[a]

Polymer	Fragment	Li^+ binding energy (eV)	ESP map	ESP minimum (eV)
PEO		-1.86		-1.92
CAR		-1.99		-1.77
SUL		-2.33		-1.90

[a]Optimized structures, binding energies, and ESPs determined at the DFT-B3LYP level of theory,[27] using Dunning's aug-cc-pVTZ basis set.[28] Details of the calculations can be found in the Supporting Information. In the structural models, cyan, gray, red, and yellow colors, respectively, correspond to hydrogen, carbon, oxygen, and sulfur atoms. The fragments are terminated using methyl groups; we assume that such a choice does not influence significantly the fragment's properties.

Polymers are constructed by alternating one ethylene oxide (EO) monomer and one secondary site, as illustrated in Figure 1. The degree of polymerization was chosen to minimize deviations to the molecular weight of PEO_{50} (2205 kDa), which we consider here as our reference. The values are reported in the left column of Figure 1. The electrolyte systems we modeled consist of 20 polymer chains and 50 lithium bis(trifluoromethanesulfonyl)imide (LiTFSI) molecules, which leads to a salt concentration of $r = 0.05$ Li^+/EO for the PEO electrolyte. Because all polymers have roughly the same molecular weight, the systems prepared have about the same molality. Random amorphous starting configurations were constructed using a Monte-Carlo scheme. For each polymer type, we considered 3−5 independent configurations, in order to randomize trajectories. All molecular dynamics simulations were run using the large atomic molecular massively parallel simulator (LAMMPS),[29] and all structural models were prepared using the MedeA simulation environment.[30]

The various interactions at play were described using the polymer consistent force-field (PCFF+).[31,32] This model covers a wide range of chemistries and has been already applied to the description of PEO/LiTFSI electrolytes.[20,33] In such a model, electrostatics were accounted for using a static point-charge model. This leads to an overestimation of the interaction between ions, which we partially

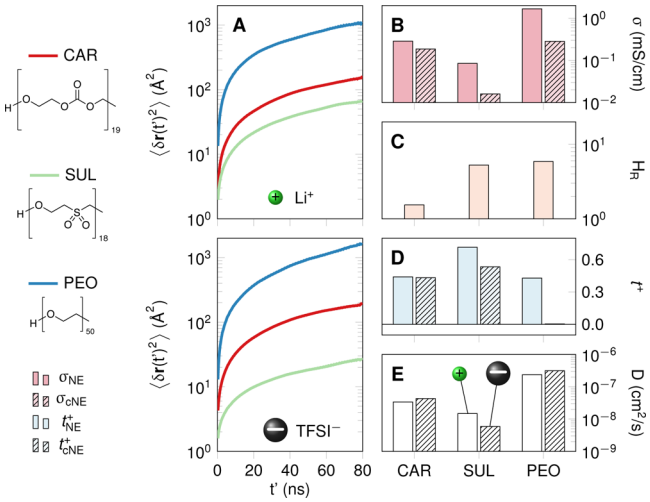

Figure 1. Transport properties of the three polymer electrolytes investigated. Left column: chemical structures. (A) Time-evolution of the mean squared displacement for Li^+ (top) and $TFSI^-$ (bottom) ions. (B) Conductivity results in the Nernst−Einstein (NE) and cluster NE (cNE) approximations. (C) Haven ratio. (D) Cation transference number as defined in both approximations. (E) Ionic diffusion coefficients.

compensate for by downscaling ions' partial charges to $|z_\pm| = 0.7$, a typical procedure for classical molecular dynamics simulations.[34−37] However, and as we will see later on, we stress that the strength of ionic interactions remains exaggerated, with an underestimation of the ionic conductivity of PEO_{50}: the results obtained are representative of higher salt concentrations. Nevertheless, this fact is of little importance to this study, as we are principally interested in *relative* differences among properties of the different polymers investigated here. We note that a more accurate description of electrostatic interactions in electrolytes can be achieved using polarizable interatomic potentials[34,38−41]—however, including these effects leads to a substantial increase in the computational cost, which translates into larger uncertainty in the properties we determine. More importantly, currently published polarizable force fields lack the chemical generality of a potential like PCFF+, which is essential to this study. Long-range Coulombic interactions have been taken into account through a particle−particle particle mesh solver with a real-space cutoff of 12 Å. Lennard-Jones interactions were truncated at a distance of 12 Å, with long-range tail corrections[42] applied to the total energy and pressure.

The relaxation process of all initial configurations consists in a sequence of energy minimizations and dynamics in the canonical (nVT) and isothermal−isobaric (nPT) statistical ensembles, for a total duration of 5 ns, at a target temperature of 363 K and pressure of 1 atm. This is the same exact relaxation sequence as the one reported by Molinari et al., for PEO/LiTFSI systems.[33] The time step was set to 0.5 fs; this value was selected as the largest one ensuring a satisfying conservation of the total energy in the microcanonical ensemble, at relevant temperatures. We have used a Nosé−Hoover thermostat and barostat, with equations of motion from Shinoda et al.,[43] using damping parameters set to 50.0 and 500.0 fs. The final volume was determined by an average over the last 500 ps of the last nPT step. The standard deviation of the volume calculated over different initial configurations was less than 0.1%. Finally, we sampled atomic displacements during 80 ns long runs in the nVT ensemble. The total sampled time, considering all independent configurations, therefore ranged between 240 and 400 ns for each polymer type. From the atomic displacements, we then computed a range of properties, including ion diffusion coefficients, NE and cNE conductivities, and their associated cation transference numbers. In the NE approximation, ions are considered as noninteracting species, which leads to deviations with respect to the exact conductivity[44−47] when ionic

DOI: 10.1021/acs.chemmater.9b02645
Chem. Mater. 2020, 32, 121−126

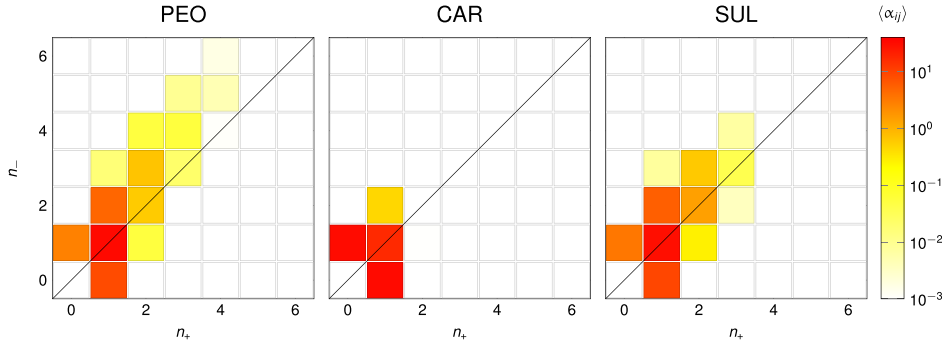

Figure 2. Ion clustering statistics in the three investigated polymer electrolytes. Notice the logarithmic scale. In PEO, a large asymmetrical distribution is observed. Addition of CARs allows enhancement of salt dissociation: the distribution mainly consists in free ions and ionic pairs. Effect from SULs is less noticeable: the distribution is slightly more symmetric, and fewer large clusters exist.

correlation is strong, for instance, at high salt concentrations or with low dielectric constant solvents. To better estimate ionic conductivity, we used a recently developed method, which accounts for the clustering of ions.[20] In this approximation (named cluster Nernst–Einstein, or cNE), clusters of ions are considered as independent species, and much more accurate estimates to the conductivity are obtained for concentrated electrolytes. More details on the specifics of our calculations are included in the Supporting Information.

■ RESULTS AND DISCUSSION

The main properties related to ion transport in an electrolyte are reported in Figure 1. First, one can see from the mean squared displacements (Figure 1A) and the diffusion coefficients (Figure 1E) that the fastest diffusion of both cations and anions occurs in the reference PEO electrolyte. In addition, the ideal and cNE conductivities (Figure 1B) are the highest in PEO. This illustrates the difficulty in finding a better polymer electrolyte than the current standard: PEO has indeed been known as a high ionic conductivity host polymer for more than 40 years.[8]

Anions are known to diffuse faster than cations in PEO[15] because of the fact that the latter interact strongly with polymer chains, effectively slowing them down. The anion, on the other hand, is loosely coordinated by the polymer, allowing for a higher mobility. Here, we obtain a $TFSI^-$ diffusion coefficient ($D_- = 3.1 \times 10^{-7}$ cm^2/s) only marginally larger than the Li^+ diffusion coefficient ($D_+ = 2.4 \times 10^{-7}$ cm^2/s), which is due to our model's overestimation of ionic interactions. As we will see later, many ionic pairs and higher order aggregates form in our simulations of PEO, which tends to bring the cation and anion diffusion coefficients together. For comparison, Hayamizu et al.[48] report diffusion coefficients measured using pulsed-field gradient spin-echo NMR under the same conditions of $D_- = 4.3 \times 10^{-7}$ cm^2/s, and $D_+ = 1.1 \times 10^{-7}$ cm^2/s. As in PEO, ions effectively diffuse roughly at the same rate in the CAR polymer electrolyte. For the SUL case, cations diffuse clearly faster than anions, which leads to a NE t^+ (i.e., the ratio between D_+ and $D_+ + D_-$, Figure 1D) larger than 0.7. Finally, the CAR and SUL polymers, respectively, show an ideal (NE) conductivity ∼6 and ∼20 times less than PEO because of overall slow diffusion of the ion.

Quite a different picture emerges when accounting for interactions between ions. We have computed the Haven ratio (reported in Figure 1C), a measure of the importance of ionic correlation, defined here as $H_R = \sigma_{NE}/\sigma_{cNE}$. In the cNE framework, it therefore corresponds to the reduction in conductivity when considering ionic clustering. As one can see, ionic correlations are significant in the PEO and SUL electrolytes ($H_R > 5.0$). Clustering therefore leads to a fivefold reduction of conductivity for PEO and SUL. On the other hand, ionic correlations seem to be much weaker in the CAR electrolyte. PEO's conductivity still is the highest in the cNE approximation ($\sigma_{cNE}^{PEO} = 0.283$ mS/cm) but is now almost matched by the CAR polymer ($\sigma_{cNE}^{CAR} = 0.186$ mS/cm). The cNE cation transference numbers also provide some interesting information. Negative transference numbers have been recently measured in PEO at high salt concentrations,[17,49] indicating a strong contribution of negatively charged clusters involving cations (i.e., the $[Li(TFSI)_2]^-$ triplet)[20,33] and in other systems including fluorinated electrolytes,[50] and salt/ionic liquid mixtures.[51] In the latter case, Molinari et al.[52] showed that neglecting ionic correlations leads to incorrect conclusions because the correct physics cannot be captured. They have also reported[53] negative transference numbers for a wide range of ionic liquid and salt combinations. Rosenwinkel and Schönhoff recently reported[54] positive cation transference numbers measured using electrophoretic NMR for a range of salt concentrations in PEO/LiTFSI. More experimental characterization is therefore needed to determine the exact degree and impact of interionic correlations in PEO electrolytes. Here, for PEO, we obtain a roughly zero t^+. For CAR and SUL, t^+ values greater than 0.4 are reached. From the divergence between the NE and cNE results, we can now clearly see how important it is to consider ionic interactions. The NE framework simply does not allow the capture of correct physics at high enough salt concentrations.

A detailed analysis of the cluster populations, reported in Figure 2 for all three polymer electrolytes, provides valuable insight concerning the mechanisms of conductivity reduction because of ionic aggregation. For PEO, our observations are consistent with previous work:[20,33] ion pairs dominate, there is a non-negligible concentration of negatively charged triplets, and the overall distribution is asymmetrical, leaning toward more anions in the clusters. This has already been well studied recently; this asymmetry finds its origin in the strong interaction between PEO and Li^+, effectively leaving less cations available to bind with loosely coordinated anions. Clustering in the CAR variant is rather different: a much larger number of free cations and anions exist, and virtually no higher order clusters are observed. Overall, more than 60% of the ions are free, most of the rest forming ion pairs. The SUL case is closer to what is observed in PEO, but the distribution is slightly more symmetrical, which could indicate that $TFSI^-$ ions interact more strongly with the SULs than with EO.

DOI: 10.1021/acs.chemmater.9b02645
Chem. Mater. 2020, 32, 121−126

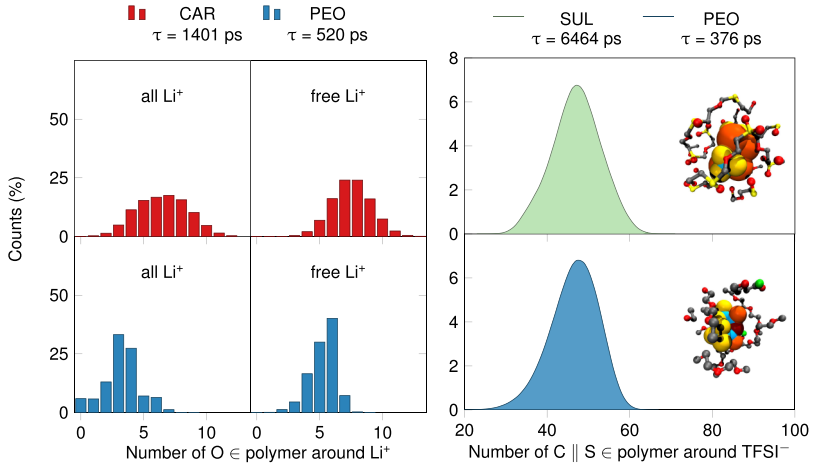

Figure 3. (Left) Li^+ and (right) $TFSI^-$ coordination contribution from polymers in three different electrolytes. In the left panel, we also report the coordination environment of a subset of all cations, the *free* Li^+, which are not coordinated by any $TFSI^-$ anion.

In order to complete the above analysis, we have probed ions' local environments in the PEO, SUL, and CAR electrolytes. These results are reported in Figure 3. We are also reporting a relaxation time τ,[55] corresponding to how long, on average, an ion remains coordinated by a given species. More details concerning the calculation of coordination environments can be found in the Supporting Information. According to the clustering analysis, we suspect a strong interaction between cations and CARs from the CAR variant; we have therefore computed the average number of oxygen (i.e., negatively charged) atoms from the polymer chains coordinating Li ions. From our coordination environment analysis, it is clear that the CAR is responsible for a tighter coordination of Li ions: on average, there are more O polymer atoms in the solvation shell of Li in CAR than in PEO. In addition, the lifetime of an Li^+−O interaction is almost three times longer in the presence of CARs. While a stronger interaction between the polymer and the cation is beneficial in reducing ionic association—and therefore in increasing conductivity—it also contributes to increasing cation-mediated cross-linking, which in turn slows down ion dynamics. This is also observed in CAR and leads to a reduction in conductivity. In amorphous polymer electrolytes, where the segmental motion of the chains drives ion diffusion, there is therefore a clear and subtle trade-off between ion association and ion mobility, which can be tuned through the binding strength between the polymer and the ions.

For the SUL polymer variant, we have studied the anion's coordination environment contribution from the polymer's positively charged atoms (C and S), compared to PEO. Both environments are similar in terms of number of coordinating atoms. However, the SUL solvation shell is significantly more static: on average, it takes an order of magnitude longer for a pair to dissociate in the SUL variant, compared to PEO. To understand this result, we have computed the interaction energy between fragments using hybrid DFT (B3LYP-aug-cc-pVTZ). The sulfone−$TFSI^-$ interaction (−0.71 eV) is twice as strong as the EO−$TFSI^-$ (−0.35 eV) one. Interaction energies calculated using the PCFF+ potential match these values very well (−0.71 and −0.32 eV). This strong affinity between the anion and the polymer consequently leads to the high t^+ observed. However, it also leads to anion-mediated cross-linking of the SUL chains, which strongly hinders dynamics.

CONCLUSIONS

In summary, we have shown in this study how the transport properties of a polymer electrolyte can be tuned using secondary sites. The chemistry of the secondary site is directly related to the nature and to the strength of its interactions with cations and anions, which eventually dictate ion diffusion coefficients, transference numbers, and the conductivity of the electrolyte. We have demonstrated how the addition of carbonate groups to the PEO backbone can significantly reduce ion pairing due to the enhanced interaction with Li cations, and how a sulfonyl secondary site will lead to a very high cation transference number, as a result of its strong affinity with $TFSI^-$. At the same time, our results emphasize the trade-off between ionic association and mobility and the difficulty of optimizing a polymer structure in order to maximize its conductivity and t^+. Finally, we have shown how important it is to go beyond the NE approximation for realistic salt concentrations, when ion−ion interactions cannot be neglected.

ASSOCIATED CONTENT

Supporting Information

The Supporting Information is available free of charge at https://pubs.acs.org/doi/10.1021/acs.chemmater.9b02645.

Quantum chemistry calculations, molecular dynamics calculations, PCFF+ partial charges, radial distribution functions, coordination environment calculations (PDF)

Configurations, input scripts, and interatomic potential parameter files in the LAMMPS format for the PEO, CAR, and SUL electrolytes (ZIP)

AUTHOR INFORMATION

Corresponding Author

*E-mail: jcg@mit.edu.

ORCID

Arthur France-Lanord: 0000-0003-0586-1945
Yanming Wang: 0000-0002-0912-681X
Tian Xie: 0000-0002-0987-4666
Jeremiah A. Johnson: 0000-0001-9157-6491
Yang Shao-Horn: 0000-0001-8714-2121
Jeffrey C. Grossman: 0000-0003-1281-2359

DOI: 10.1021/acs.chemmater.9b02645
Chem. Mater. 2020, 32, 121−126

Notes

The authors declare no competing financial interest.

■ ACKNOWLEDGMENTS

This work was supported by the Toyota Research Institute (TRI). The computational support was provided by the Extreme Science and Engineering Discovery Environment, supported by National Science Foundation grant number ACI-1053575, and by the National Energy Research Scientific Computing Center, a DOE Office of Science User Facility supported by the Office of Science of the U.S. Department of Energy under contract no. DE-AC02-05CH11231.

■ REFERENCES

(1) Xu, K. Nonaqueous liquid electrolytes for lithium-based rechargeable batteries. *Chem. Rev.* **2004**, *104*, 4303−4418.
(2) Xu, K. Electrolytes and interphases in Li-ion batteries and beyond. *Chem. Rev.* **2014**, *114*, 11503−11618.
(3) Meyer, W. H. Polymer electrolytes for lithium-ion batteries. *Adv. Mater.* **1998**, *10*, 439−448.
(4) Stephan, A. M. Review on gel polymer electrolytes for lithium batteries. *Eur. Polym. J.* **2006**, *42*, 21−42.
(5) Agrawal, R. C.; Pandey, G. P. Solid polymer electrolytes: materials designing and all-solid-state battery applications: an overview. *J. Phys. D: Appl. Phys.* **2008**, *41*, 223001.
(6) Song, J. Y.; Wang, Y. Y.; Wan, C. C. Review of gel-type polymer electrolytes for lithium-ion batteries. *J. Power Sources* **1999**, *77*, 183−197.
(7) Bachman, J. C.; Muy, S.; Grimaud, A.; Chang, H.-H.; Pour, N.; Lux, S. F.; Paschos, O.; Maglia, F.; Lupart, S.; Lamp, P.; et al. Inorganic solid-state electrolytes for lithium batteries: mechanisms and properties governing ion conduction. *Chem. Rev.* **2015**, *116*, 140−162.
(8) Wright, P. V. Electrical conductivity in ionic complexes of poly(ethylene oxide). *Br. Polym. J.* **1975**, *7*, 319−327.
(9) Lopez, J.; Mackanic, D. G.; Cui, Y.; Bao, Z. Designing polymers for advanced battery chemistries. *Nat. Rev. Mater.* **2019**, *4*, 312.
(10) Pesko, D. M.; Webb, M. A.; Jung, Y.; Zheng, Q.; Miller, T. F., III; Coates, G. W.; Balsara, N. P. Universal relationship between conductivity and solvation-site connectivity in ether-based polymer electrolytes. *Macromolecules* **2016**, *49*, 5244−5255.
(11) Cha, E. H.; Macfarlane, D. R.; Forsyth, M.; Lee, C. W. Ionic conductivity studies of polymeric electrolytes containing lithium salt with plasticizer. *Electrochim. Acta* **2004**, *50*, 335−338.
(12) Fan, L.-Z.; Maier, J. Composite effects in poly (ethylene oxide)−succinonitrile based all-solid electrolytes. *Electrochem. Commun.* **2006**, *8*, 1753−1756.
(13) Echeverri, M.; Kim, N.; Kyu, T. Ionic conductivity in relation to ternary phase diagram of poly (ethylene oxide), succinonitrile, and lithium bis (trifluoromethane) sulfonimide blends. *Macromolecules* **2012**, *45*, 6068−6077.
(14) Xue, Z.; He, D.; Xie, X. Poly(ethylene oxide)-based electrolytes for lithium-ion batteries. *J. Mater. Chem. A* **2015**, *3*, 19218−19253.
(15) Gorecki, W.; Jeannin, M.; Belorizky, E.; Roux, C.; Armand, M. Physical properties of solid polymer electrolyte PEO (LiTFSI) complexes. *J. Phys.: Condens. Matter* **1995**, *7*, 6823.
(16) Pożyczka, K.; Marzantowicz, M.; Dygas, J.; Krok, F. Ionic conductivity and lithium transference number of poly (ethylene oxide): LiTFSI system. *Electrochim. Acta* **2017**, *227*, 127−135.
(17) Pesko, D. M.; Timachova, K.; Bhattacharya, R.; Smith, M. C.; Villaluenga, I.; Newman, J.; Balsara, N. P. Negative transference numbers in poly (ethylene oxide)-based electrolytes. *J. Electrochem. Soc.* **2017**, *164*, E3569−E3575.
(18) Doeff, M. M.; Georèn, P.; Qiao, J.; Kerr, J.; De Jonghe, L. Transport Properties of a High Molecular Weight Poly (propylene oxide)-LiCF3 SO 3 System. *J. Electrochem. Soc.* **1999**, *146*, 2024−2028.
(19) Xie, T.; France-Lanord, A.; Wang, Y.; Shao-Horn, Y.; Grossman, J. C. Graph dynamical networks for unsupervised learning of atomic scale dynamics in materials. *Nat. Commun.* **2019**, *10*, 2667.
(20) France-Lanord, A.; Grossman, J. C. Correlations from Ion Pairing and the Nernst-Einstein Equation. *Phys. Rev. Lett.* **2019**, *122*, 136001.
(21) Doyle, M.; Fuller, T. F.; Newman, J. The importance of the lithium ion transference number in lithium/polymer cells. *Electrochim. Acta* **1994**, *39*, 2073−2081.
(22) Ma, Q.; Zhang, H.; Zhou, C.; Zheng, L.; Cheng, P.; Nie, J.; Feng, W.; Hu, Y.-S.; Li, H.; Huang, X.; et al. Single lithium-ion conducting polymer electrolytes based on a super-delocalized polyanion. *Angew. Chem., Int. Ed.* **2016**, *55*, 2521−2525.
(23) Qiao, B.; Leverick, G. M.; Zhao, W.; Flood, A. H.; Johnson, J. A.; Shao-Horn, Y. Supramolecular Regulation of Anions Enhances Conductivity and Transference Number of Lithium in Liquid Electrolytes. *J. Am. Chem. Soc.* **2018**, *140*, 10932−10936.
(24) Liu, W.; Liu, N.; Sun, J.; Hsu, P.-C.; Li, Y.; Lee, H.-W.; Cui, Y. Ionic Conductivity Enhancement of Polymer Electrolytes with Ceramic Nanowire Fillers. *Nano Lett.* **2015**, *15*, 2740−2745.
(25) Lee, S.-I.; Schömer, M.; Peng, H.; Page, K. A.; Wilms, D.; Frey, H.; Soles, C. L.; Yoon, D. Y. Correlations between Ion Conductivity and Polymer Dynamics in Hyperbranched Poly(ethylene oxide) Electrolytes for Lithium-Ion Batteries. *Chem. Mater.* **2011**, *23*, 2685−2688.
(26) Savoie, B. M.; Webb, M. A.; Miller, T. F., III Enhancing cation diffusion and suppressing anion diffusion via Lewis-acidic polymer electrolytes. *J. Phys. Chem. Lett.* **2017**, *8*, 641−646.
(27) Stephens, P. J.; Devlin, F. J.; Chabalowski, C. F.; Frisch, M. J. Ab Initio Calculation of Vibrational Absorption and Circular Dichroism Spectra Using Density Functional Force Fields. *J. Phys. Chem.* **1994**, *98*, 11623−11627.
(28) Dunning, T. H. Gaussian basis sets for use in correlated molecular calculations. I. The atoms boron through neon and hydrogen. *J. Chem. Phys.* **1989**, *90*, 1007−1023.
(29) Plimpton, S. Fast parallel algorithms for short-range molecular dynamics. *J. Comput. Phys.* **1995**, *117*, 1−19.
(30) *MedeA-2.22*; Materials Design, Inc: San Diego, CA USA, 2018.
(31) Sun, H. Force field for computation of conformational energies, structures, and vibrational frequencies of aromatic polyesters. *J. Comput. Chem.* **1994**, *15*, 752−768.
(32) Rigby, D.; Sun, H.; Eichinger, B. E. Computer simulations of poly (ethylene oxide): force field, pvt diagram and cyclization behaviour. *Polym. Int.* **1997**, *44*, 311−330.
(33) Molinari, N.; Mailoa, J. P.; Kozinsky, B. Effect of Salt Concentration on Ion Clustering and Transport in Polymer Solid Electrolytes: A Molecular Dynamics Study of PEO−LiTFSI. *Chem. Mater.* **2018**, *30*, 6298−6306.
(34) Borodin, O.; Smith, G. D. Structure and Dynamics of N-Methyl-N-propylpyrrolidinium Bis(trifluoromethanesulfonyl)imide Ionic Liquid from Molecular Dynamics Simulations. *J. Phys. Chem. B* **2006**, *110*, 11481−11490.
(35) Youngs, T. G. A.; Hardacre, C. Application of Static Charge Transfer within an Ionic-Liquid Force Field and Its Effect on Structure and Dynamics. *ChemPhysChem* **2008**, *9*, 1548−1558.
(36) Lynden-Bell, R. M.; Youngs, T. G. A. Simulations of imidazolium ionic liquids: when does the cation charge distribution matter? *J. Phys.: Condens. Matter* **2009**, *21*, 424120.
(37) Rigby, J.; Izgorodina, E. I. Assessment of atomic partial charge schemes for polarisation and charge transfer effects in ionic liquids. *Phys. Chem. Chem. Phys.* **2013**, *15*, 1632−1646.
(38) Borodin, O.; Smith, G. D.; Douglas, R. Force Field Development and MD Simulations of Poly(ethylene oxide)/LiBF4 Polymer Electrolytes. *J. Phys. Chem. B* **2003**, *107*, 6824−6837.
(39) Borodin, O.; Smith, G. D. Development of Many-Body Polarizable Force Fields for Li-Battery Components: 1. Ether, Alkane, and Carbonate-Based Solvents. *J. Phys. Chem. B* **2006**, *110*, 6279−6292.

DOI: 10.1021/acs.chemmater.9b02645
Chem. Mater. 2020, 32, 121−126

(40) Starovoytov, O. N.; Borodin, O.; Bedrov, D.; Smith, G. D. Development of a Polarizable Force Field for Molecular Dynamics Simulations of Poly (Ethylene Oxide) in Aqueous Solution. *J. Chem. Theory Comput.* **2011**, *7*, 1902−1915.
(41) Bauschlicher, C. W.; Haskins, J. B.; Bucholz, E. W.; Lawson, J. W.; Borodin, O. Structure and Energetics of Li+(BF4-)n, Li+(FSI-)n, and Li+(TFSI-)n: Ab Initio and Polarizable Force Field Approaches. *J. Phys. Chem. B* **2014**, *118*, 10785−10794.
(42) Sun, H. COMPASS: an ab initio force-field optimized for condensed-phase applications overview with details on alkane and benzene compounds. *J. Phys. Chem. B* **1998**, *102*, 7338−7364.
(43) Shinoda, W.; Shiga, M.; Mikami, M. Rapid estimation of elastic constants by molecular dynamics simulation under constant stress. *Phys. Rev. B: Condens. Matter Mater. Phys.* **2004**, *69*, 134103.
(44) Carbone, L.; Gobet, M.; Peng, J.; Devany, M.; Scrosati, B.; Greenbaum, S.; Hassoun, J. Polyethylene glycol dimethyl ether (PEGDME)-based electrolyte for lithium metal battery. *J. Power Sources* **2015**, *299*, 460−464.
(45) Carbone, L.; Munoz, S.; Gobet, M.; Devany, M.; Greenbaum, S.; Hassoun, J. Characteristics of glyme electrolytes for sodium battery: nuclear magnetic resonance and electrochemical study. *Electrochim. Acta* **2017**, *231*, 223−229.
(46) Carbone, L.; Verrelli, R.; Gobet, M.; Peng, J.; Devany, M.; Scrosati, B.; Greenbaum, S.; Hassoun, J. Insight on the Li 2 S electrochemical process in a composite configuration electrode. *New J. Chem.* **2016**, *40*, 2935−2943.
(47) Marcolongo, A.; Marzari, N. Ionic correlations and failure of Nernst-Einstein relation in solid-state electrolytes. *Phys. Rev. Mater.* **2017**, *1*, 025402.
(48) Hayamizu, K.; Akiba, E.; Bando, T.; Aihara, Y. 1 H, 7 Li, and 19 F nuclear magnetic resonance and ionic conductivity studies for liquid electrolytes composed of glymes and polyetheneglycol dimethyl ethers of CH 3 O (CH 2 CH 2 O) n CH 3 (n= 3−50) doped with LiN (SO 2 CF 3) 2. *J. Chem. Phys.* **2002**, *117*, 5929−5939.
(49) Villaluenga, I.; Pesko, D. M.; Timachova, K.; Feng, Z.; Newman, J.; Srinivasan, V.; Balsara, N. P. Negative Stefan-Maxwell Diffusion Coefficients and Complete Electrochemical Transport Characterization of Homopolymer and Block Copolymer Electrolytes. *J. Electrochem. Soc.* **2018**, *165*, A2766−A2773.
(50) Shah, D. B.; Nguyen, H. Q.; Grundy, L. S.; Olson, K. R.; Mecham, S. J.; DeSimone, J. M.; Balsara, N. P. Difference between approximate and rigorously measured transference numbers in fluorinated electrolytes. *Phys. Chem. Chem. Phys.* **2019**, *21*, 7857−7866.
(51) Gouverneur, M.; Schmidt, F.; Schönhoff, M. Negative effective Li transference numbers in Li salt/ionic liquid mixtures: does Li drift in the "Wrong" direction? *Phys. Chem. Chem. Phys.* **2018**, *20*, 7470−7478.
(52) Molinari, N.; Mailoa, J. P.; Craig, N.; Christensen, J.; Kozinsky, B. Transport anomalies emerging from strong correlation in ionic liquid electrolytes. *J. Power Sources* **2019**, *428*, 27−36.
(53) Molinari, N.; Mailoa, J. P.; Kozinsky, B. General Trend of Negative Li Effective Charge in Ionic Liquid Electrolytes. *J. Phys. Chem. Lett.* **2019**, *10*, 2313.
(54) Rosenwinkel, M. P.; Schönhoff, M. Lithium Transference Numbers in PEO/LiTFSA Electrolytes Determined by Electrophoretic NMR. *J. Electrochem. Soc.* **2019**, *166*, A1977−A1983.
(55) Brehm, M.; Kirchner, B. TRAVIS - A Free Analyzer and Visualizer for Monte Carlo and Molecular Dynamics Trajectories. *J. Chem. Inf. Model.* **2011**, *51*, 2007−2023.

DOI: 10.1021/acs.chemmater.9b02645
Chem. Mater. 2020, 32, 121−126